Dependence of Vibration Direction of Shear Wave in Ultrasonic Transmission Defect Detection

Takeru Doi[1‡], Ryusuke Miyamoto[2], Naoto Wakatsuki[1], Tadashi Ebihara[1], Koichi Mizutani[1] ([1]Univ. Tsukuba; [2]Tokyo Univ. of Marine Sci. & Tech.)

1. Introduction

Billets, the primary steel product, are manufactured by continuous casting. If the defects induced by the casting process are left in the following process, the defects are stretched and become larger. The enlargement of defects deteriorates the quality of material, and it may result in the damage of the final products. Therefore, it is well-known that non-destructive testing using ultrasonic waves has the primary importance to detect internal defects in steel billets because of its simplicity and safety advantages [1].

Previous studies have investigated transmission methods using longitudinal ultrasound [2,3]. The authors have conducted research on the usefulness of shear ultrasound in the detection of defects by the transmission method [4,5]. In previous studies [4,5], defect detection using time-of-flight with shear waves has been found to detect defects to the same level as longitudinal waves. Furthermore, verification in the vibration directions shown in **Table 1** (1), (2), (7), (8) shows that the increase of time-of-flight changes when the shear waves are injected in different vibration directions [4]. In this paper, we verify through simulations how the transmitted wave changes with the presence of defects when the vibration direction of the shear wave is changed between the transmitter and receiver as shown in (3)-(6) of Table 1.

2. Simulation Condition

Figure 1 shows a schematic of the 3D simulation. We use finite-difference-time-domain (FDTD) method. The testing billet is assumed to be a duralumin (A2017), whose density is 2,730 kg/m³, longitudinal wave velocity is 6,206 m/s, and shear wave velocity is 3,126 m/s. The size of the billet is 100×100×100 (mm²). The mesh size was set to 0.25 mm, so the mesh space was 401×401×401, and the time discrete width was set to 23.3 ns. A cylindrical defect of 2 mm diameter is placed in the center of the billet extending along the z-axis. The aperture diameter of the transmitter and receiver is 10 mm, the position of the transmitter is fixed at $x = 50$ (mm) in the x-axis and $y = 50$ (mm) in the y-axis in Fig.1, and the receiver is placed on the opposite side to receive the propagated ultrasonic waves. As shown in Fig. 1, the sensitivity axis in the x-axis direction and the sensitivity axis in the z-axis direction and the defects are transmitted and received in the combinations (1) to (8) in Table 1. The transmitted ultrasound wave was a sine burst wave expressed in Equation (1). We set the frequency f to 1.56 Mhz in order to make the wavelength of the shear wave equal to the diameter of the defect, which is 2 mm. In addition, T was set to approximately 2.6 μs to transmit 4 waves, and the 40 μs received waveform was measured.

$$s(t) = \sin(2\pi f t)\ [0 \le t \le T] \qquad (1)$$

Table 1 Combination of vibration direction for transmitting and receiving shear waves and defect direction.

	Shear sensitivy axis of Transmitter	Defect	Receiver	
(1)	x		x	Previous Study
(2)	x	z	x	Previous Study
(3)	x		z	Current Study
(4)	x	z	z	Current Study
(5)	z		x	Current Study
(6)	z	z	x	Current Study
(7)	z		z	Previous Study
(8)	z	z	z	Previous Study

Longitudinal Direction of Defect x : x-axis, z : z-axis

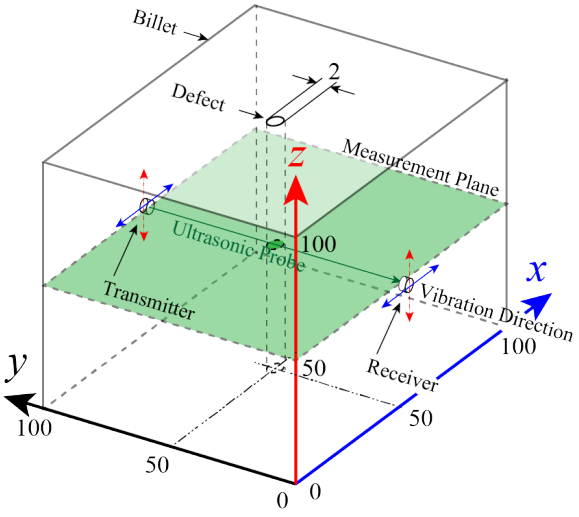

Fig.1 Schematic diagram of simulation conditions for billet measurement.

doi@aclab.esys.tsukuba.ac.jp
wakatuki@iit.tsukuba.ac.jp

3. Simulation Results

Figure 2 shows the transmitted waveform used in the simulation and the results of received waveforms with different combinations of vibration directions as shown in Table 1 at x = 50 mm and y = 50 mm. In Fig.2, the waveforms were normalized based on the maximum values of (1) ~ (8). The gray zone in the figure is the received waveform when there is no defect, and the white zone is the received waveform when there is a defect. From previous studies, it is known that results (1), (2), (7), and (8) are caused by changes in the arrival time of sound waves, and these changes in propagation time are used to detect defects [4]. In (3) and (5) of Fig. 2, it was found that no signal was received. This is because the displacement and sensitivity axis are perpendicular to each other, so no signal is detected. In both cases of (4) and (6), the defect may cause scattered waves. In the case of (4), the incident wave, which vibrates in x-direction, was scattered by the defect. The scattered wave may have the vibration direction in x-y plane. Thus, it has the vibration in x-direction at the receiver position. However, since the receiver has the sensitivity axis of z direction, no signal was received. In the similar manner in the case of (6), no signal was received. They are valid results. In future simulations, we would like to simulate under conditions that are outside of the symmetry. In addition, as a future prospect, we would like to consider the case of vibration direction is tilted from the longitudinal direction of defects.

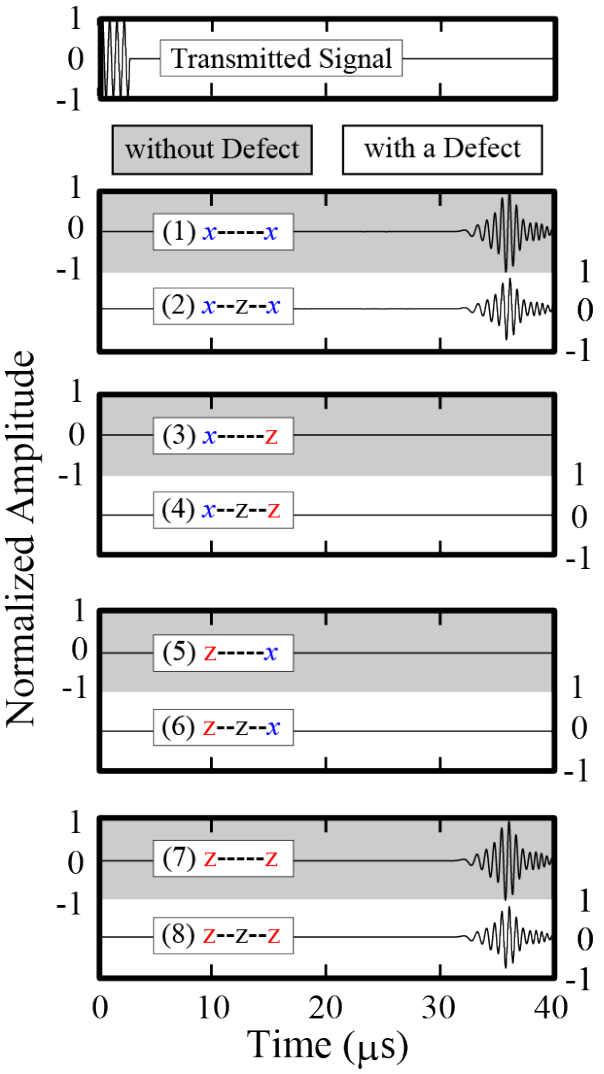

Fig. 2 Simulation results of received waveforms for combinations of vibration directions in Table 1.

4. Conclusions

In this study, we verified using three-dimensional simulations how the received waveform changes when the vibration direction of the shear wave ultrasound is changed vertically between the transmitter and the receiver with respect to a cylindrical defect extending in one direction. As a result, when the axis of sensitivity of the shear wave on the receiver side was changed by 90 degrees to the transmitter, amplitude was not received either with or without a defect in the propagation path, but this may be improved by eliminating the symmetry. Future studies include verification of what kind of mode conversion occurs when shear waves are transmitted at an angle to the direction of the defect through experiments.

References

1. R. K. Gupta *et al.,* Eng. Failure Anal., **13** (2005).
2. H. Mitsui *et al*., Jpn. J. Appl. Phys., **48** (2009) 07GD05.
3. H. Mitsui *et al*., Jpn. J. Appl. Phys. **50**, 116601 (2011).
4. T Doi *et al.,* Proc. 42nd Symp. Ultrasonic Electronics (2021) 1Pa2-5.
5. T Doi *et al.,* Jpn. J. Appl. Phys. **61** (2022) SG1039.